Micropatterning Thermoplasmonic Gold Nanoarrays To Manipulate Cell Adhesion

Min Zhu,[†,‡] Guillaume Baffou,[§] Nikolaus Meyerbröker,[⊥] and Julien Polleux[†,*]

[†]Department of Molecular Medicine, Max Planck Institute of Biochemistry, 82152 Martinsried, Germany, [‡]State Key Laboratory of High Performance Ceramics and Superfine Microstructure, Shanghai Institute of Ceramics, Chinese Academy of Sciences, 1295 Ding-Xi Road, Shanghai, 200050, People's Republic of China, [§]Fresnel Institute, CNRS, Aix-Marseille Université, Ecole Centrale Marseille, Campus de St Jérôme, 13013 Marseille, France, and [⊥]Angewandte Physikalische Chemie, Universität Heidelberg, Im Neuenheimer Feld 253, 69120 Heidelberg, Germany

ABSTRACT The ability to reversibly control the interactions between the extracellular matrix (ECM) and cell surface receptors such as integrins would allow one to investigate reciprocal signaling circuits between cells and their surrounding environment. Engineering microstructured culture substrates functionalized with switchable molecules remains the most adopted strategy to manipulate surface adhesive properties, although these systems exhibit limited reversibility and require sophisticated preparation procedures. Here, we report a straightforward protocol to fabricate biofunctionalized micropatterned gold nanoarrays that favor one-dimensional cell migration and function as plasmonic nanostoves to physically block and orient the formation of new adhesion sites. Being reversible and not restricted spatiotemporally, thermoplasmonic approaches will open new opportunities to further study the complex connections between ECM and cells.

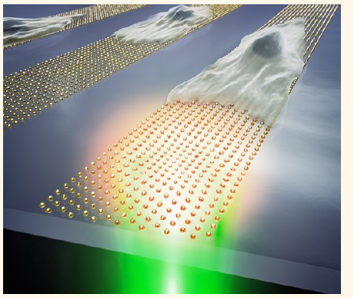

KEYWORDS: block copolymer micellar lithography · deep UV lithography · thermoplasmonics · cell adhesion · nanobiotechnology

Analysis of cell behavior by exogenously controlling cellular processes with the help of biophysical means represents a complementary approach to classic methods, such as gene knockdown[1] and pharmacological strategies.[2] Reversible manipulation of interactions between the extracellular matrix (ECM) and cell surface receptors such as integrins would allow cell adhesion to be specifically triggered, allowing one to systematically analyze reciprocal signaling circuits between cells and their surrounding environment. The combination of micro/nanofabrication with stimulus-responsive surface chemistries has proven to be a versatile tool to modify extracellular environments at the single cell level. External stimuli such as voltage and light can switch on or off the adhesive properties of surface-anchored molecules to dissect new aspects of cell adhesion,[3,4] detachment,[5] and migration.[6,7] However, limitations regarding advanced fabrication procedures, stimulus localization, and binding reversibility limit the applicability of chip-based devices and their transfer from bioengineering to cell biology laboratories.[8] To overcome such issues, the development of new strategies is critical.

Variations in culture medium temperature can be used to release cells when cultured onto dishes functionalized with thermo-responsive polymers, but this approach is considered invasive because the adhesive properties of the whole substrate are changed.[9] To make use of temperature in a less invasive manner, electrically heated microwire electrodes were utilized to induce cellular release of heat-shock proteins.[10] Such an approach to manipulate allosteric interactions between cells and their binding environment has not been attempted due to the restricted spatial freedom in generating local heat.

Gold nanoparticles can act as heat nanosources when excited at their plasmonic resonance due to enhanced light absorption. Thermoplasmonics and related photothermal effects have opened a new realm of biological applications in nanotechnology,[11] including the engineering of optofluidic systems,[12,13] analysis of DNA dissociation,[14] selective destruction of cancerous cells,[15,16] and the intracellular release of bioactive molecules.[17] So far, these applications exclusively used dispersed nanoparticles rather than immobilized ones, which would allow for the design of functional platforms to manipulate cell adhesion.

Here, we report a straightforward protocol to fabricate biofunctionalized micropatterned gold nanoarrays that support integrin-mediated adhesion and function as

* Address correspondence to polleux@biochem.mpg.de.

Received for review May 26, 2012 and accepted July 18, 2012.

Published online July 18, 2012
10.1021/nn302329c

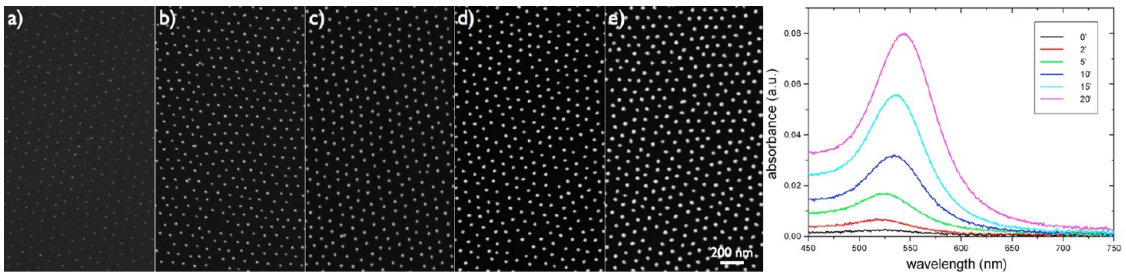

Figure 1. Ethanolamine-assisted growth of gold nanoparticles supported on glass coverslips. Scanning electron microscopy (SEM) images of gold nanoarrays after immersion for (a) 0, (b) 5, (c) 10, (d) 15, and (e) 20 min in an aqueous solution of ethanolamine (2 mM) and $KAuCl_4$ (0.1 wt %). Right: Absorption spectra of the different gold nanoarrays displayed by the SEM images.

plasmonic nanostoves to physically block and orient the formation of new adhesion sites.

RESULTS AND DISCUSSION

Although many techniques are available for the fabrication of nanoparticle-based devices, they all have significant shortcomings in using benchtop facilities, minimizing the number of preparation steps, and controlling independently the structural parameters of the device. Among various advanced lithographic techniques, block copolymer micellar lithography (BCML) has been recognized as a straightforward method for generating a wide variety of periodic nanostructures with long-range order.[18,19] Although interparticle distance can be adjusted from 25 to 250 nm, control over particle diameter is restricted to sizes below 10 nm. Here, we used quasi-hexagonally organized gold nanoarrays with a separation distance of about 90 nm and a particle diameter of 7 nm. As such nanostructured surfaces do not exhibit an intense absorption band for effective photothermal effects, an additional step is needed to grow larger gold particles. Hydroxylamine seeding of colloidal gold[20] was shown to be applicable to gold nanoarrays upon functionalizing the substrate with alkyl chains to prevent particles from spontaneously lifting off during size enlargement.[18] To avoid this laborious substrate modification step, we directly immersed glass-supported gold nanoarrays into an aqueous solution of Au^{3+} and tested, for the first time, the use of ethanolamine as a reducing agent. Since alkylamines can mediate the generation of gold nanoparticles while acting as dual capping and reducing agents,[21] we chose ethanolamine because of its water solubility. As displayed in Figure 1, we successfully applied ethanolamine-mediated seeding of colloidal gold onto nanoarrays, in which the particle diameter homogeneously increased from 7 to 32 nm in 20 min and the plasmon band intensity centered at 530 nm became significantly stronger.

To make these nanostructures compatible with cell-based experiments, we first passivated the glass background with poly(ethylene glycol) (PEG) and functionalized the gold particles with a cysteine-terminated linear arginine-glycine-aspartic acid (RGD) polypeptide.[22] RGD is a conserved motif found in several ECM proteins, such as fibronectin. RGD epitopes are bound by transmembrane receptors of the integrin family, which mediate adhesion and physically connect the cytoskeleton to the ECM.[23,24] In tissue culture, cells migrate on these uniform surfaces in random directions. To restrict their migration path, which can in turn affect properties such as migration speed and cell morphology, it is possible to confine cells onto defined areas by using micropatterned substrates coated with ECM proteins. For instance, cell migration on thin fibronectin-coated lines was shown to be similar to *in vivo*-like situations where migration occurs faster and more persistently than on standard unpatterned culture substrates.[25] To apply this concept to our setup, we decided to restrict gold nanoparticle distribution to 10 μm wide lines in order to confine cell adhesion to one dimension.

To prepare micropatterned gold nanoarrays, other lithography techniques must be combined with BMCL. For instance, electron-beam lithography allows the local immobilization of deposited gold-loaded micelles onto a substrate upon emitting a beam of electrons in a patterned fashion across the specimen.[26] Despite a patterning precision of 100 nm, this method necessitates a scanning electron microscope and long processing rates. More commonly, parallel procedures, such as photolithography and microcontact deprinting, are used to more effectively fabricate patterns larger than 1 μm.[27−29] However, these advanced protocols still hinder the high sample throughput necessary for biological screening experiments. In an effort to remain affordable and minimize the number of processing steps, we applied the simplicity of a serial approach in a parallel fashion by using deep ultraviolet (UV) illumination on gold-loaded micellar monolayers. With a wavelength of 185 nm, deep UV lithography can directly photoconvert chemical groups without using photosensitizers and cross-linkers.[30] Here, we successfully prepared micropatterned gold nanoparticles by illuminating micellar monolayers with deep UV through a quartz photomask and transferring the substrate to toluene to remove non-irradiated micelles (Figure 2). As revealed by X-ray photoelectron spectroscopy (Figure S1 in the Supporting Information),

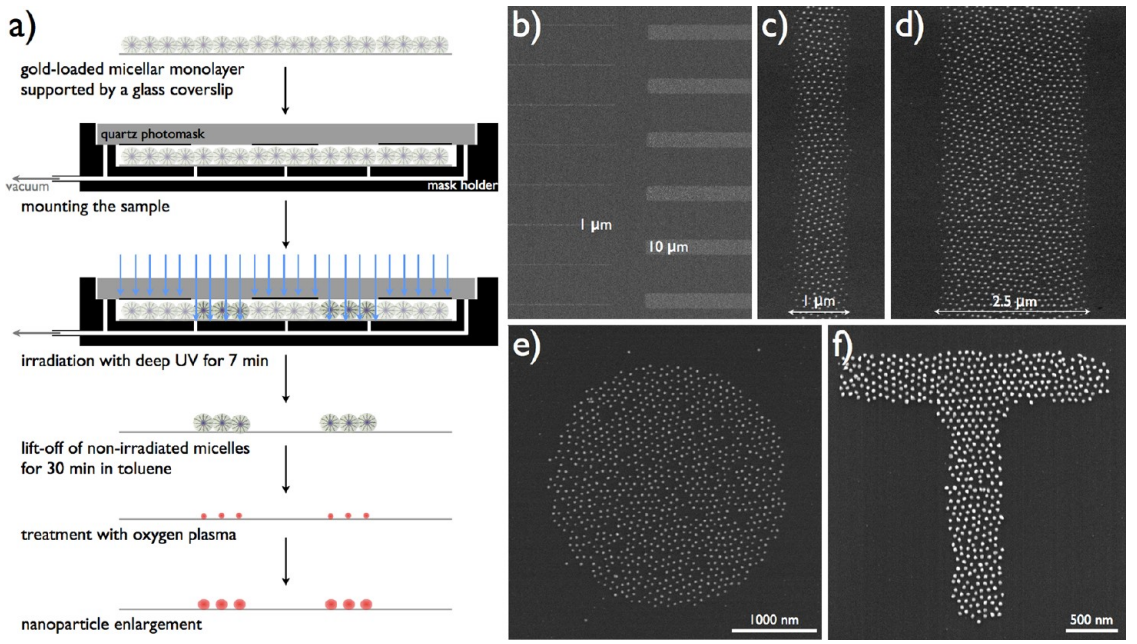

Figure 2. Combining deep ultraviolet lithography and micellar nanolithography to micropattern thermoplasmonic gold nanoarrays. (a) Schematic diagram illustrating the successive steps necessary to fabricate micropatterned gold nanoparticles. (b) Low-magnification SEM image of nanostructured lines with widths of 1 and 10 μm. (c–f) High-resolution SEM images of micropatterned gold nanoarrays of various shapes and dimensions.

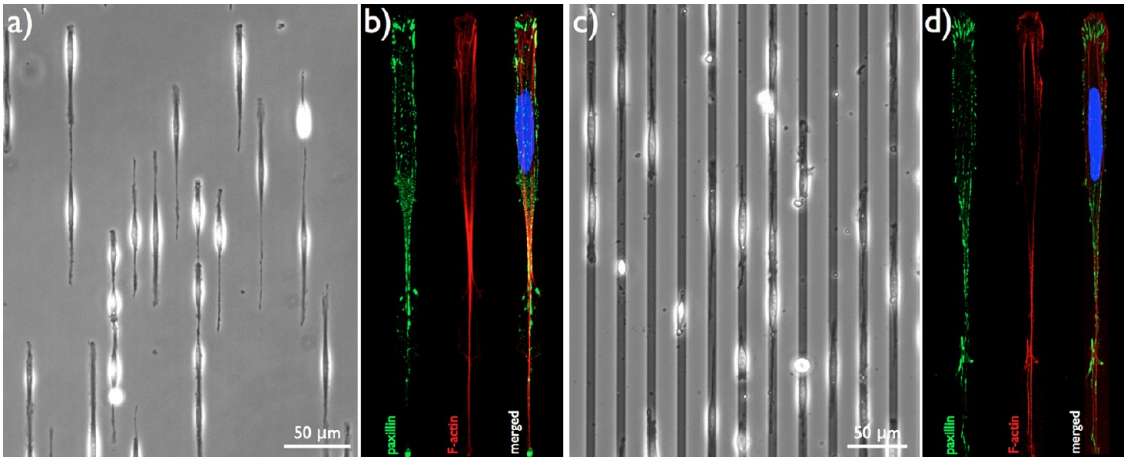

Figure 3. Cell adhesion on fibronectin- (FN) and arginine-glycine-aspartic acid (RGD)-coated 10 μm wide lines occurs similarly. Phase contrast microscopy images of mouse fibroblasts migrating onto (a) FN-coated glass and (c) RGD-functionalized gold nanoparticles of 35 nm in diameter separated by 90 nm. Confocal fluorescence microscopy images of fixed cells expressing green fluorescent protein (GFP)-labeled paxillin and stained for filamentous F-actin (in red) displaying, respectively, adhesive sites and cytoskeleton of a cell migrating onto (b) FN-coated glass and (d) RGD-coated gold nanoparticles.

the immobilization of micelles occurred by partially oxidizing their polystyrene shells with deep UV, which enhances their affinity to the glass substrate and reduces their solubility in toluene. As displayed in Figure 2, this approach can rapidly micropattern gold nanoparticles into various geometries and feature sizes of about 500 nm, while conserving their quasi-hexagonal organization.

Next, we seeded mouse fibroblasts onto 10 μm wide lines of biofunctionalized 35 nm gold particles separated by passivated glass. Similarly as on fibronectin-coated lines, fibroblasts selectively adhered to the linear RGD-functionalized gold nanoarrays and adopted a polarized shape to initiate migration without modifying the structure of gold nanoarrays (Figures 3 and S2). By staining filamentous actin (F-actin) and paxillin, an adaptor protein that connects the actin cytoskeleton to the cytoplasmic tail of integrins, it can be observed that cells display similar intracellular architecture on both types of substrates, as revealed by confocal fluorescence microscopy (Figure 3).

Besides confining the migration path of fibroblasts, micropatterned gold nanoarrays have the ability to generate heat when illuminated with a laser beam at a wavelength $\lambda = 532$ nm, where the plasmon resonance

peak is centered. In contrast to electrically heated microwires, the use of thermoplasmonic structures provides more spatial freedom, as control over thermal variations depends not only on pattern geometry but also on laser position. Temperature measurements were performed by quadriwave shearing interferometry (TIQSI), a recent thermal imaging technique based on thermal-induced variation of the refractive index of the liquid environment (*cf.* Experimental Methods).[31] By imaging heat profiles with this technique, we found that temperature increases proportionally with laser power. Although the laser beam displays a homogeneous power density, we measured thermal variations of 12.8, 18.7, and 24.2 K at the beam center and 7.5, 13, and 16.7 K at its periphery for 2, 3, and 4 mW output powers, respectively (Figure 4). The temperature variations follow a parabolic profile within the illumination area which decreases by $1/R$ outside the beam.[31] Since many cellular components absorb visible light, we minimized the risk of phototoxicity by taking advantage of the temperature variations that occur outside the direct illumination area to manipulate cells.

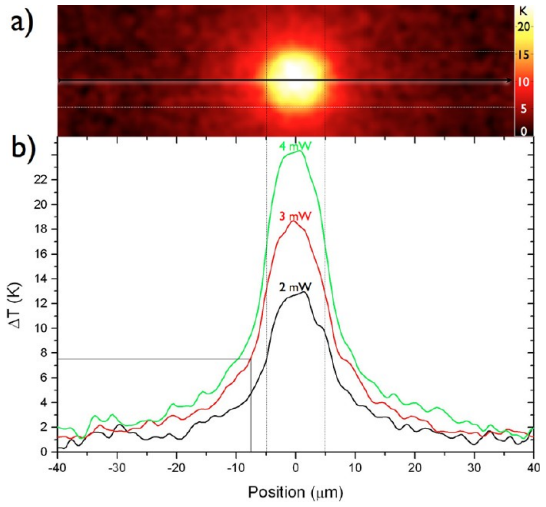

Figure 4. Photothermal effects of a quasi-hexagonal lattice of spherical gold nanoparticles under laser illumination at a wavelength λ = 532 nm. The measurements were performed on gold nanoarrays (diameter 35 nm, interdistance 90 nm) during illumination with a beam of 10 μm in diameter at powers of 2, 3, and 4 mW. (a) Temperature distribution released by the nanostructures exposed to a laser power of 4 mW. (b) Temperature profile obtained from the linescan (black arrow in (a)) drawn on the temperature map at laser powers of 2, 3, and 4 mW. The white dashed lines indicate the borders of the 10 μm wide lines made of gold particles.

We tested the ability of local heat to interfere with cell adhesion by simultaneously blocking and guiding protrusive activity during cell spreading and migration. For this purpose, we first modified an epifluorescence microscope by replacing the excitation lamp with a green diode laser (Figure S3). Upon seeding fibroblasts, we first monitored cell spreading with live-cell imaging in different conditions (Figure 5a–c and movie 1 in Supporting Information). Without the laser, the cell spread equally in both directions for 30 min and finally polarized to initiate migration (Figure 5a). By illuminating an area adjacent to the cell with a laser beam of about 3 mW, the generation of local heat blocked the

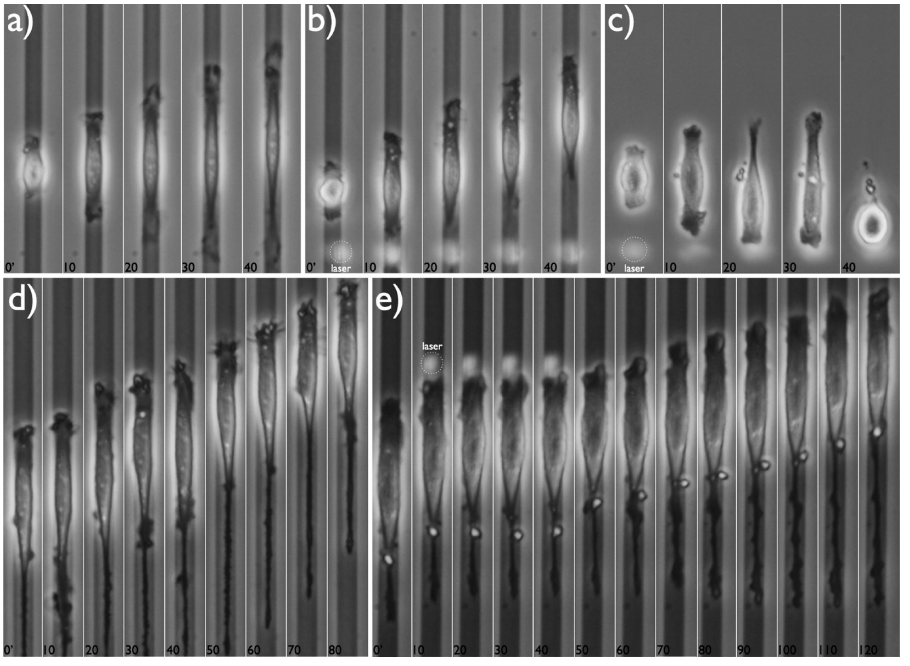

Figure 5. Heat-assisted manipulation of cell adhesion during spreading and migration. Guided cell migration during spreading: phase contrast images of cells spreading onto RGD-coated nanoparticles of 35 nm in diameter (a) without and (b) with laser illumination of 3 mW for 40 min. (c) Cell spreading onto RGD-coated glass coverslip under the same irradiation conditions as in (b). Blocking cell adhesion during migration: phase contrast images of cells migrating onto RGD-coated particles (d) without and (e) with laser illumination of 3 mW for 30 min. Each image has a time interval of 10 min.

formation of adhesion sites in one direction and allowed protrusive activity in the opposite direction, inducing the cell to polarize and initiate migration earlier (Figure 5b). To confirm that the effect on cell behavior is due to heat, we immobilized RGD epitopes onto micropatterned PEG-coated glass, which does not absorb green light and therefore does not generate heat (Figure 5c). With the same illumination conditions as previously used, the cell spontaneously spread within the irradiated area, emphasizing that light alone does not stop the formation of adhesion sites, whereas heat can. Moreover, this experiment illustrates the phototoxicity caused by laser illumination in the longer term, which prevents the cell from migrating over the beam and induces cell death within 20 min.

As a second example of cell manipulation, migrating cells could also be stopped for up to 30 min by local heat generation, acting similarly as a wall (Figure 5d,e and movie 2 in Supporting Information). Upon turning the laser illumination off, cells instantly reinitiated migration in the direction of the prior illumination, which emphasizes the reversible character of thermoplasmonic manipulations.

According to Figure 4, the cell periphery experiences a local temperature of about 44 °C when localized 2.5 μm away from the beam border. To compare the effect of local and global heat on new adhesion site formation, we seeded fibroblasts on RGD-functionalized gold nanoarrays at 37 and 44 °C (Figure S4). In comparison to cells cultured at 37 °C (Figure S4b), we observed that cells neither adhered to the substrate at 44 °C during the first 30 min nor managed to normally spread the following hour. Moreover, by cooling the culture medium to 37 °C after 90 min in culture at 44 °C, cells did not recover their ability to effectively adhere (Figure S4a). It is difficult to interpret these observations in the context of cell adhesion since many proteins other than integrins can be denatured at 44 °C. In contrast to global heat, thermoplasmonic manipulation operates more locally and does not disable cells to adapt their behavior depending on local temperature. Possible effects of local heat on cell adhesion include the weakening of integrin−RGD interactions and/or the denaturation of integrins and the cell membrane. Although a temperature of 44 °C corresponds to an extreme physiological condition, it is important to note that cells neither died nor lost their ability to migrate persistently after local heat exposure.

CONCLUSION

In the present study, we report a simple and cost-effective protocol to micropattern thermoplasmonic nanoarrays by combining deep UV and micellar lithography. Being reversible and not restricted spatiotemporally, the generation of photothermal gradients in the vicinity of cells interferes locally with cell adhesion and allows both guiding and blocking cell migration in a defined microenvironment. As a future challenge, it will be crucial to extend the use of deep UV-assisted micellar nanolithography to designing gold structures that absorb wavelengths within the tissue transparency window, such as near-infrared. By overcoming cellular phototoxicity and fluorophore photobleaching, thermoplasmonic manipulation could be performed while analyzing live-cell spreading, migration, and detachment by fluorescence microscopy. Moreover, this approach could be applied to spatiotemporally manipulate the affinities of other cell surface receptors to their respective ligands, which would enable one to further dissect reciprocal signaling circuits between cells and their environment.

EXPERIMENTAL METHODS

Fabrication of Extended Gold Nanoarrays. In a typical synthesis, polystyrene(1056)-*block*-poly(2-vinylpyridine)(495) (PS_{1056}-*b*-$P2VP_{495}$) from Polymer Source Inc. was dissolved at room temperature in anhydrous toluene (Sigma-Aldrich) at a concentration of 5 mg/mL and stirred for 2 days. The quantity of gold precursor was calculated relative to the number of P2VP units (N_{P2VP}) with a loading parameter (L) equal to 0.5, that is, 1 molecule of $HAuCl_4$ for 2 P2VP monomers. Hydrogen tetrachloroaurate(III) trihydrate ($HAuCl_4 \cdot 3H_2O$, Sigma-Aldrich) was added to the polymer solution and stirred for 2 days in a sealed glass vessel. Glass coverslips (Carl Roth) were cleaned in a piranha solution for at least 5 h and were extensively rinsed with Milli-Q water and dried under a stream of nitrogen. Gold-loaded micellar monolayers were prepared by dip-coating a glass coverslip into the previously prepared solutions with a constant velocity equal to 24 mm·min^{-1}. To remove the organic template and form inorganic nanoparticles, the dip-coated glass slides were exposed to oxygen plasma (150 W, 0.15 mbar, 45 min, PVA TEPLA 100 Plasma System). Scanning electron measurements were performed with a dual beam (FIB/SEM) instrument (Quanta 3D FEG, FEI, Hillsboro).

Fabrication of Micropatterned Gold Nanoarrays. This protocol is schematically described in Figure 2. Briefly, a glass coverslip coated with a gold-loaded micellar monolayer was immobilized with vacuum onto a mask holder and then sandwiched with a photomask made of a patterned chromium layer supported on UV-transparent quartz (ML&C, Jena). The system was then exposed to deep UV light using a low-pressure mercury lamp (Heraeus Noblelight GmbH, NIQ 60/35 XL long-life lamp, quartz tube, 60 W) at 5 cm distance for 7 min. The micellar monolayer was then incubated for 30 min in toluene to wash non-irradiated micelles away and dried with the hood airflow. The enlargement of immobilized gold nanoparticles was performed by incubating the substrate for several minutes in 10 mL of an aqueous solution containing ethanolamine (2 mM) and $KAuCl_4$ (0.1 wt %).

Surface Functionalization. Gold nanoarrays supported on glass coverslips were incubated in water with 0.25 mg/mL of poly-(L-lysine)-*g*-poly(ethylene glycol) PLL-*g*-PEG (SuSoS) for 2 h. The substrates were rinsed with water, dried with nitrogen, and incubated for 5 h in a 50 μM aqueous solution of fibronectin-mimicking polypeptide, N-terminated C-L_3G_3PHRSN-G_6-RGDS.[32] Finally, the substrates were rinsed and incubated overnight in water before plating fibroblasts.

Thermal Imaging of Micropatterned Gold Nanoarrays[31]. Temperature measurements were performed by quadriwave shearing interferometry (TIQSI), a recent thermal imaging technique based on thermal-induced variation of the refractive index of the liquid environment. More precisely, due to the thermal-induced generation of refractive index gradients in the heated region, the optical

wavefront of an incident light beam that passes through the sample experiences a distortion. This wavefront distortion is imaged using a Hartmann grating in front of a CCD camera. The interferogram recorded by the CCD camera is then numerically processed to retrieve the actual temperature distribution using a deconvolution algorithm. This approach is particularly simple since it is label-free and it allows rapidly and quantitatively mapping a temperature distribution with an accuracy of less than 1 K.

Setup for Thermoplasmonic Manipulation. In order to microlocally generate heat while performing live-cell imaging, we equipped a Zeiss Axiovert 40 CFL microscope (Carl Zeiss, Jena, Germany) with a cell culture chamber (37 °C, 5% CO_2), a green laser (Laserglow, Hercules 250, $\lambda = 532$ nm), a beam splitter, a band-pass filter, and a camera (Canon, EOS 450D), as depicted in Figure S4. For cell manipulation experiments, approximately 1×10^6 cells in DMEM containing 0.5% FBS were seeded onto functionalized micropatterned gold nanoarrays. Thermoplasmonic experiments were conducted within the following 10 h to avoid the contribution of ECM secretion.

Immunofluorescence. Fibroblasts were incubated for 3 h in culture, then fixed with 2% paraformaldehyde, permeabilised with 0.1% Triton X-100, and incubated with primary and secondary antibodies. Paxillin was stained with antipaxillin (mouse monoclonal; Transduction Laboratories), F-actin with phalloidin (Molecular Probes), and nuclei with DAPI. Secondary antibodies used for immunofluorescence were from Invitrogen (Alexa488, Alexa647). The fluorescent images were collected by laser scanning confocal microscopy (TCS SP5; Leica) with a 63× oil objective and Leica confocal software.

Conflict of Interest: The authors declare no competing financial interest.

Acknowledgment. We thank R. Fässler for support, and K. Legate and H.B. Schiller for careful reading of the manuscript. The 7th Framework Program of the European Community (FP7) through the Marie Curie Action for career development (IEF—"Multi-PGNAs"), MPG CAS joint doctoral promotion program (DPP), and the Max Planck Society financially supported this work.

Supporting Information Available: Supplementary methods; X-ray photoelectron spectroscopy analysis; additional low- and high-magnification SEM images, schematics of microscope setup used for thermoplasmonic manipulation and movie legends. This material is available free of charge *via* the Internet at http://pubs.acs.org.

REFERENCES AND NOTES

1. Vicente-Manzanares, M.; Ma, X.; Adelstein, R. S.; Horwitz, A. R. Non-Muscle Myosin II Takes Centre Stage in Cell Adhesion and Migration. *Nat. Rev. Mol. Cell Biol.* **2009**, *10*, 778–790.
2. Fenteany, G.; Zhu, S. Small-Molecule Inhibitors of Actin Dynamics and Cell Motility. *Curr. Top. Med. Chem.* **2003**, *3*, 593–616.
3. Collier, J.; Mrksich, M. Engineering a Biospecific Communication Pathway between Cells and Electrodes. *Proc. Natl. Acad. Sci. U.S.A.* **2006**, *103*, 2021–2025.
4. Nakanishi, J.; Kikuchi, Y.; Inoue, S.; Yamaguchi, K.; Takarada, T.; Maeda, M. Spatiotemporal Control of Migration of Single Cells on a Photoactivatable Cell Microarray. *J. Am. Chem. Soc.* **2007**, *129*, 6694–6695.
5. Wildt, B.; Wirtz, D.; Searson, P. C. Programmed Subcellular Release for Studying the Dynamics of Cell Detachment. *Nat. Methods* **2009**, *6*, 211–213.
6. Jiang, X.; Bruzewicz, D. A.; Wong, A. P.; Piel, M.; Whitesides, G. M. Directing Cell Migration with Asymmetric Micropatterns. *Proc. Natl. Acad. Sci. U.S.A.* **2005**, *102*, 975–978.
7. Rolli, C. G.; Nakayama, H.; Yamaguchi, K.; Spatz, J. P.; Kemkemer, R.; Nakanishi, J. Switchable Adhesive Substrates: Revealing Geometry Dependence in Collective Cell Behavior. *Biomaterials* **2012**, *33*, 2409–2418.
8. Robertus, J.; Browne, W. R.; Feringa, B. L. Dynamic Control over Cell Adhesive Properties Using Molecular-Based Surface Engineering Strategies. *Chem. Soc. Rev.* **2010**, *39*, 354.
9. Nagase, K.; Kobayashi, J.; Okano, T. Temperature-Responsive Intelligent Interfaces for Biomolecular Separation and Cell Sheet Engineering. *J. R. Soc. Interface* **2009**, *6*, S293–S309.
10. Ginet, P.; Montagne, K.; Akiyama, S.; Rajabpour, A.; Taniguchi, A.; Fujii, T.; Sakai, Y.; Kim, B.; Fourmy, D.; Volz, S. Towards Single Cell Heat Shock Response by Accurate Control on Thermal Confinement with an On-Chip Microwire Electrode. *Lab Chip* **2011**, *11*, 1513.
11. Baffou, G.; Quidant, R. Thermo-Plasmonics: Using Metallic Nanostructures as Nano-Sources of Heat. *Laser Photonics Rev.* **2012**, early view.
12. Liu, G. L.; Kim, J.; Lu, Y.; Lee, L. P. Optofluidic Control Using Photothermal Nanoparticles. *Nat. Mater.* **2006**, *5*, 27–32.
13. Donner, J. S.; Baffou, G.; McCloskey, D.; Quidant, R. Plasmon-Assisted Optofluidics. *ACS Nano* **2011**, *5*, 5457–5462.
14. Stehr, J.; Hrelescu, C.; Sperling, R. A.; Raschke, G.; Wunderlich, M.; Nichtl, A.; Heindl, D.; Kurzinger, K.; Parak, W. J.; Klar, T. A.; Feldmann, J. Gold Nanostoves for Microsecond DNA Melting Analysis. *Nano Lett.* **2008**, *8*, 619–623.
15. Hirsch, L.; Stafford, R.; Bankson, J.; Sershen, S.; Rivera, B.; Price, R.; Hazle, J.; Halas, N.; West, J. Nanoshell-Mediated Near-Infrared Thermal Therapy of Tumors under Magnetic Resonance Guidance. *Proc. Natl. Acad. Sci. U.S.A.* **2003**, *100*, 13549–13554.
16. El-Sayed, I.; Huang, X.; El-Sayed, M. Surface Plasmon Resonance Scattering and Absorption of Anti-EGFR Antibody Conjugated Gold Nanoparticles in Cancer Diagnostics: Applications in Oral Cancer. *Nano Lett.* **2005**, *5*, 829–834.
17. Huschka, R.; Neumann, O.; Barhoumi, A.; Halas, N. J. Visualizing Light-Triggered Release of Molecules Inside Living Cells. *Nano Lett.* **2010**, *10*, 4117–4122.
18. Lohmueller, T.; Aydin, D.; Schwieder, M.; Morhard, C.; Louban, I.; Pacholski, C.; Spatz, J. P. Nanopatterning by Block Copolymer Micelle Nanolithography and Bioinspired Applications. *Biointerphases* **2011**, *6*, MR1–MR12.
19. Polleux, J.; Rasp, M.; Louban, I.; Plath, N.; Feldhoff, A.; Spatz, J. P. Benzyl Alcohol and Block Copolymer Micellar Lithography: A Versatile Route to Assembling Gold and *In Situ* Generated Titania Nanoparticles into Uniform Binary Nanoarrays. *ACS Nano* **2011**, *5*, 6355–6364.
20. Brown, K.; Lyon, L.; Fox, A.; Reiss, B.; Natan, M. Hydroxylamine Seeding of Colloidal Au Nanoparticles. 3. Controlled Formation of Conductive Au Films. *Chem. Mater.* **2000**, *12*, 314–323.
21. Aslam, M.; Fu, L.; Su, M.; Vijayamohanan, K.; Dravid, V. P. Novel One-Step Synthesis of Amine-Stabilized Aqueous Colloidal Gold Nanoparticles. *J. Mater. Chem.* **2004**, *14*, 1795.
22. Arnold, M.; Cavalcanti-Adam, E.; Glass, R.; Blummel, J.; Eck, W.; Kantlehner, M.; Kessler, H.; Spatz, J. Activation of Integrin Function by Nanopatterned Adhesive Interfaces. *ChemPhysChem* **2004**, *5*, 383–388.
23. Polleux, J. *Bioactive Surfaces. Interfacing Cell Surface Receptors to Hybrid Nanopatterned Surfaces: A Molecular Approach for Dissecting the Adhesion Machinery*; Börner, H. G., Lutz, J. F., Eds.; Springer-Verlag: Berlin, 2011; Vol. 240, pp 79–102.
24. Takahashi, S.; Leiss, M.; Moser, M.; Ohashi, T.; Kitao, T.; Heckmann, D.; Pfeifer, A.; Kessler, H.; Takagi, J.; Erickson, H. P.; *et al.* The RGD Motif in Fibronectin Is Essential for Development but Dispensable for Fibril Assembly. *J. Cell Biol.* **2007**, *178*, 167–178.
25. Doyle, A. D.; Wang, F. W.; Matsumoto, K.; Yamada, K. M. One-Dimensional Topography Underlies Three-Dimensional Fibrillar Cell Migration. *J. Cell Biol.* **2009**, *184*, 481–490.
26. Spatz, J.; Chan, V.; Mossmer, S.; Kamm, F.; Plettl, A.; Ziemann, P.; Moller, M. A Combined Top-Down/Bottom-Up Approach to the Microscopic Localization of Metallic Nanodots. *Adv. Mater.* **2002**, *14*, 1827–1832.
27. Aydin, D.; Schwieder, M.; Louban, I.; Knoppe, S.; Ulmer, J.; Haas, T. L.; Walczak, H.; Spatz, J. P. Micro-Nanostructured Protein Arrays: A Tool for Geometrically Controlled Ligand Presentation. *Small* **2009**, *5*, 1014–1018.

28. Chen, J.; Mela, P.; Moeller, M.; Lensen, M. C. Microcontact Deprinting: A Technique To Pattern Gold Nanoparticles. *ACS Nano* **2009**, *3*, 1451–1456.
29. Gorzolnik, B.; Mela, P.; Moeller, M. Nano-Structured Micropatterns by Combination of Block Copolymer Self-Assembly and UV Photolithography. *Nanotechnology* **2006**, *17*, 5027–5032.
30. Azioune, A.; Storch, M.; Bornens, M.; Thery, M.; Piel, M. Simple and Rapid Process for Single Cell Micro-Patterning. *Lab Chip* **2009**, *9*, 1640–1642.
31. Baffou, G.; Bon, P.; Savatier, J.; Polleux, J.; Zhu, M.; Merlin, M.; Rigneault, H.; Monneret, S. Thermal Imaging of Nanostructures by Quantitative Optical Phase Analysis. *ACS Nano* **2012**, *6*, 2452–2458.
32. Ebara, M.; Yamato, M.; Aoyagi, T.; Kikuchi, A.; Sakai, K.; Okano, T. A Novel Approach to Observing Synergy Effects of PHSRN on Integrin-RGD Binding Using Intelligent Surfaces. *Adv. Mater.* **2008**, *20*, 3034–3038.